CREEP RESISTANT FERRITIC STEELS FOR POWER PLANTS

Ingo von Hagen and Walter Bendick

Mannesmann Forschungsinstitut GmbH
Ehinger Strasse 200
47259 Duisburg, Germany

Abstract

The development of power plant technology towards larger units and higher efficiencies is linked to the development of creep resistant ferritic steels. Starting with simple CMn- steels, creep strength has improved successively by introducing new alloying elements and new microstructures. Niobium has been one of the most successful new elements. It is contained in all the latest high strength steels belonging to the group of 9-12% Cr- steels. The use of these steels allows the design of power plants with steam temperatures up to 625°C. As a further step ferritic steels are currently under development for maximum steam temperatures of 650°C, which is believed to be the limit that can be achieved for this group of steels.

Introduction

Creep resistant steels have been used in technical applications for many years. History shows that there has been a fruitful interaction between advances in technology and advances in the development of new steels. New steels had to be developed to put new concepts into practice, and on the other hand new technological concepts were stimulated by the availability of new steels.

Creep resistant steels are mainly used in power generating and petrochemical plants. All product forms are included. Large forgings and castings are used to build turbines, whereas tubes, pipes, plates and fittings are the typical products for application in pressure vessels, boilers and piping systems. In addition to high creep strength other material properties are also important, e.g. hardenability, corrosion resistance, and weldability. The importance of such properties depends on the specific application. For example, good hardenability is very important for a steel used for large turbine rotors, whereas good weldability is a prerequisite for an application in power plant tubing and piping. Although the different requests from application are reflected by differences in chemical composition, all product forms use the same mechanisms to improve creep strength. The large variety of creep resistant ferritic steel may therefore be covered adequately by an overview of steels used for tubing and piping.

The major driving force behind the development of power plant technology has been the requirement for improved economic efficiency. Design improvements as well as the application of new steels with better properties were used in the past to meet this requirement. Figure 1 shows the efficiency increase for hard-coal-fired power plants from 1930 until the present days.
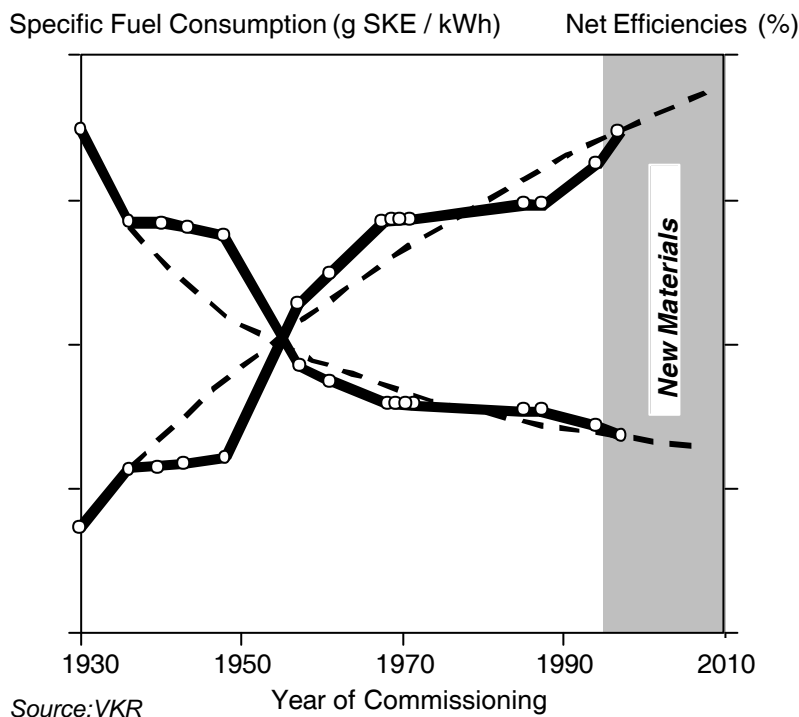

Figure 1: Increase of net efficiencies in hard-coal-fired power plants.

The fuel consumption per kWh has decreased by a factor of 2.6 within that time period. This implies an equivalent increase in plant efficiency and a decrease of CO_2 emission per kWh,

which is becoming a more and more important issue. The increased efficiency is not described by a smooth curve. It is interesting to note that the kinks in the curve reflect the introduction of a new type of creep resistant steel. Currently we are in such a phase, where efficiency increases due to the recent development of new steels.

Overview on Creep Resistant Ferritic Steels

Table I gives an overview on creep resistant ferritic steels which are used in power plants for tubing and piping. The list of steels can be subdivided into CMn- steels (No.1&2), Mo- steels (No.3&4), low alloyed CrMo- steels (No.5-9), and 9-12%Cr- steels (No.10-15). Because of the large number of different steel grades, only a few typical representatives of each group could be included in the table. In general the new European (EN-) steel designations have been used. Whenever it was possible, the comparable ASTM grade is also given. Some of the newer steel grades have only been included in ASTM and not yet in the European standards.

The steel grades have been listed according to increasing content of alloying elements. And the chemical composition becomes increasingly complex. As can be seen from Table I, niobium has been an important element. Niobium bearing steels are found in each group. It has been added for different purposes, as will be discussed later.

The complexity of chemical composition is reflected by a complexity in microstructure. Different hardening mechanisms have been used to achieve an optimised product. As a result the creep rupture strength could have been raised by a factor of about 10 (Figure 2). A more detailed characterization of strength properties of the various steels will be given in following.
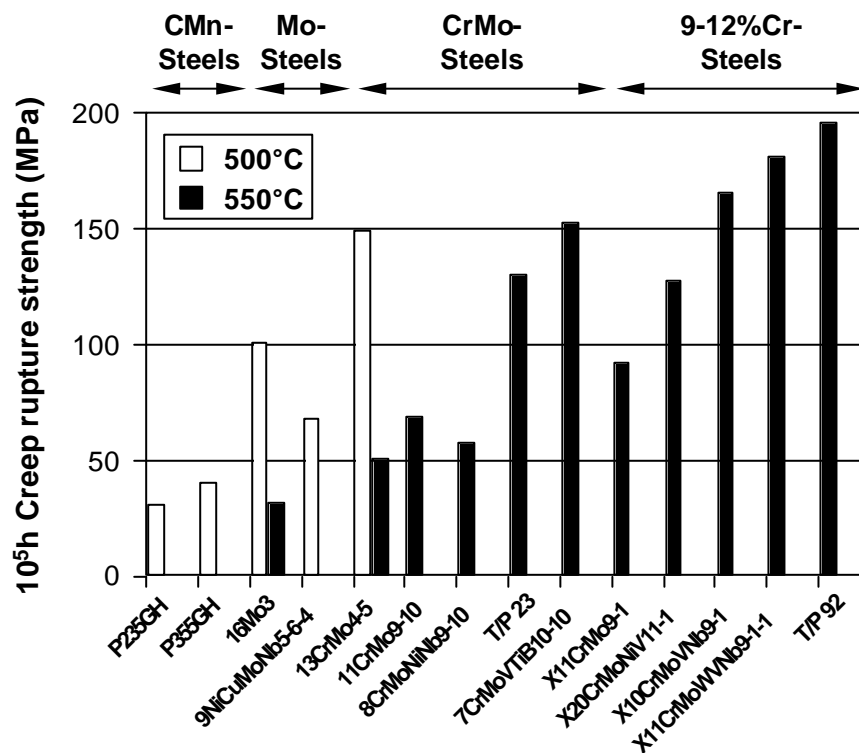

Figure 2: Creep rupture strength of heat resistant steels for tubes and pipes.

Table I Chemical compositions of creep resistant ferritic steels for power plants

No.	EN-Designation	Comparable ASTM Grade	Chemical Composition (mass-%)													
			C	Si	Mn	Al	Cu	Cr	Ni	Mo	W	Ti	V	Nb	B	N
1	P 235	A	max. 0.16	max. 0.35	0.40 −0.80	min. 0.020	max. 0.30	max. 0.30	max. 0.30	max. 0.08						
2	P 355		max. 0.22	0.15 −0.35	1.00 −1.50	max. 0.060								0.015 −0.10		
3	16Mo3		0.12 −0.20	0.15 −0.35	0.40 −0.80	max. 0.040				0.25 −0.35						
4	9NiCuMoNb5-6-4		max. 0.17	0.25 −0.50	0.80 −1.20	max. 0.050	0.50 −0.80	max. 0.30	1.00 −1.30	0.25 −0.50				0.015 −0.045		
5	13CrMo4-5	T/P11	0.10 −0.17	0.10 −0.35	0.40 −0.70	max. 0.040		0.70 −1.10		0.45 −0.65						
6	11CrMo9-10	T/P22	0.08 −0.15	0.15 −0.40	0.30 −0.70	max. 0.040		2.00 −2.50		0.90 −1.20						
7	8CrMoNiNb9-10		max. 0.10	0.15 −0.50	0.40 −0.80	max. 0.050		2.00 −2.50	0.30 −0.80	0.90 −1.10				min. 10x%C		
8	7CrMoVTiB10-10	T/P24	0.05 −0.10	0.15 −0.45	0.30 −0.70	max. 0.020		2.20 −2.60		0.90 −1.10		0.05 −0.10	0.20 −0.30		0.0015 −0.007	max. 0.010
9		T/P23	0.04 −0.10	max. 0.50	0.10 −0.60	max. 0.030		1.90 −2.60		0.05 −0.30	1.45 −1.75		0.20 −0.30	0.02 −0.08	0.0005 −0.006	max. 0.030
10	X11CrMo9-1	T/P9	0.08 −0.15	0.25 −1.00	0.30 −0.60	max. 0.040		8.0 −10.0		0.90 −1.00						
11	X20CrMoNiV11-1		0.17 −0.23	0.15 −0.50	max. 1.00	max. 0.040		10.0 −12.5	0.30 −0.80	0.80 −1.20			0.25 −0.35			
12	X10CrMoVNb9-1	T/P91	0.08 −0.12	0.20 −0.50	0.30 −0.60	max. 0.040		8.00 −9.50	max. 0.40	0.85 −1.05			0.18 −0.25	0.06 −0.10		0.030 −0.070
13	X11CrMoWVNb9-1-1	T/P911	0.09 −0.13	0.10 −0.50	0.30 −0.60	max. 0.040		8.50 −9.50	0.10 −0.40	0.90 −1.10	0.90 −1.10		0.18 −0.25	0.06 −0.10	0.0005 −0.005	0.050 −0.090
14		T/P92	0.07 −0.13	max. 0.50	0.30 −0.60	max. 0.040		8.50 −9.50	max. 0.40	0.30 −0.60	1.50 −2.00		0.15 −0.25	0.04 −0.09	0.001 −0.006	0.030 −0.070
15		T/P122	0.07 −0.13	max. 0.50	max. 0.70	max. 0.040	0.30 −1.70	10.0 −12.5	max. 0.50	0.25 −0.60	1.50 −2.50		0.15 −0.30	0.04 −0.10	max. 0.005	0.040 −0.100

CMn- Steels

Steel grade P 235 can be regarded as typical of a CMn- steel having a ferrite perlite microstructure. The carbon and manganese contents are the major factors influencing the strength properties. Figure 3 shows a plot of the minimum 0.2%- proof strength values together with the average 10^5h- creep rupture strength as function of temperature. The European design codes are based on minimum proof strength values at low and creep rupture strength values at high temperatures. Both regimes are separated by the intersection of the proof strength with the creep rupture strength curve. In the case of P 235 the intersection point is around 420°C. Above this temperature design becomes time dependent, because the lifetime of a component is limited by the creep process.

An interesting modification of P 235 is the niobium bearing grade P 355. The proof strength values could be raised considerably as a result of niobium addition due to grain refinement. However, the increase of creep rupture strength is rather small. This increase can be attributed mainly to the increase of manganese, which is a solution hardening element. Since proof and creep rupture strength have not increased by equal amounts, the intersection point between the creep and proof strength regime is shifted to 400°C. The advantage of P 355 clearly lies in the application below this temperature.
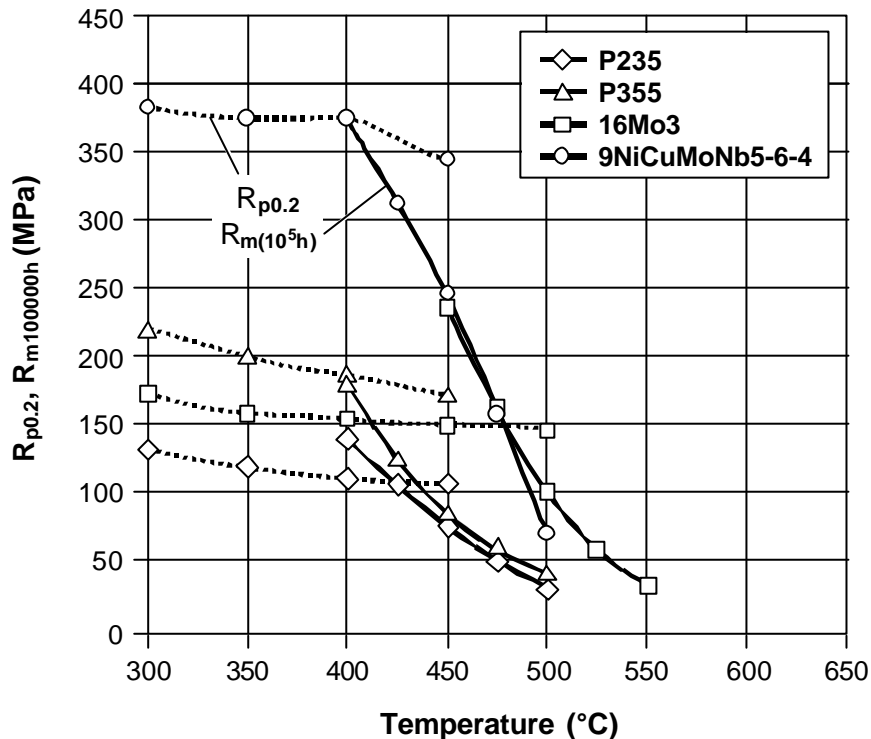

Figure 3: Strength properties of CMn- and Mo- steels.

Mo- Steels

A similar effect can also be seen for the Mo- steels, which are also represented in Figure 3. These steels are basically of the same type with about 0.3% molybdenum, which is a strong solution hardening element. The solution hardening effect is the main cause for the increase of creep rupture strength, which is similar for both steels. Grade 9NiCuMoNb5-6-4, also well known as WB 36, shows a dramatic increase of proof strength, which again is partly caused by the grain-refining effect of niobium. In addition hardening by copper precipitation increases the proof strength.

CrMo- Steels

It has been found that the strengthening effect of molybdenum cannot fully be used, since creep ductility strongly decreases with increasing molybdenum content. Another limitation in the application of Mo- steels is the observed decomposition of iron carbides above 500°C (graphitization). A solution to both problems was the use of chromium as an alloying element in combination with molybdenum. In fact CrMo- steels were the first ones that allowed steam temperatures in power stations above 500°C.

The classical CrMo- steels are 13CrMo4-5 (T/P11) and 11CrMo9-10 (T/P22). Their creep rupture strengths are distinctly higher than the simple Mo- steels (Figure 4), which is mainly a result of higher Mo- content. CrMo steels form chromium carbides which are stable above 500°C. Therefore graphitization is no longer a problem. Chromium also promotes the use at higher temperatures due to its positive influence on oxidation resistance.

The steels 7CrMoVTiB10-10 (T/P24) and T/P23, also represented in Figure 4, reveal extremely high strength properties. These are newly developed steels on the basis of T/P22. Having a similar microstructure as T/P22, their strengths properties have been raised considerably by additional alloying with titanium, vanadium and boron in the case of T/P24 as well as tungsten, vanadium, niobium and boron in T/P23. More details on the use and properties of those steels will be given later.
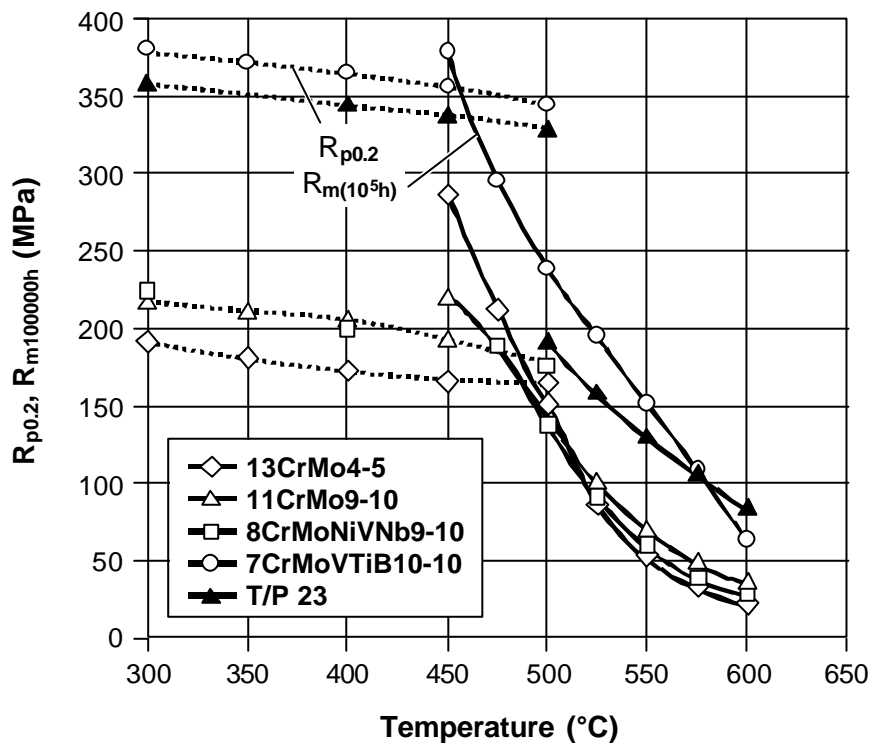

Figure 4: Strength properties of CrMo- steels.

Another interesting steel of this group is 8CrMoNiNb9-10. This is also a niobium bearing steel which reflects another facet of its use in creep resistant ferritic steels. The steel has been developed for nuclear applications in liquid sodium cooled fast breeder reactors. A problem has arisen from the use of low chromium ferritic steels, like T/P22, in combination with high chromium austenitic steels. The higher carbon affinity of the high chromium austenitic steel caused a massive diffusion of carbon from the ferritic steel via the liquid sodium into the austenitic steel. As a result a strong decrease of strength occurred in the ferritic steel and an

embrittlement in the austenitic steel. The problem was solved by alloying T/P22 with niobium leading to the formation of niobium carbides instead of chromium carbides. The stronger affinity of carbon to niobium prevents a carbon depletion of the ferritic steel and consequently a decrease in strength.

9-12% Cr- Steels

The increase of chromium in CrMo- steels above 7% leads to a group of steels which have a martensitic microstructure as common feature. This microstructure introduces a new element of structural hardening. It is characterized by a high dislocation density and a fine martensite lath structure which is stabilized by $M_{23}C_6$ precipitates. Thus structural hardening is responsible for the large increase in strength of X11CrMo9-1, as compared to 11CrMo9-10 (Figure 5). Further improvements of especially the creep strength have been achieved by alloying with vanadium, niobium, tungsten and boron. The introduction of X20CrMoNiV11-1 at the beginning of the sixties has been a major step to increase power plant efficiency (1), which can clearly be seen in Figure 1. Its creep rupture strength at a temperature of 540°C is nearly twice that of the low-alloy ferritic steels available at that time (e.g. 10CrMo9-10 with a 10^5h- creep rupture strength of 78 MPa compared to 147 MPa for X20CrMoNiV11-1). Transformation behavior and microstructure is comparable to X11CrMo9-1. The higher creep rupture strength of X20CrMoNiV11-1 is mainly caused by the higher amount of $M_{23}C_6$ carbides as caused by the higher carbon content.
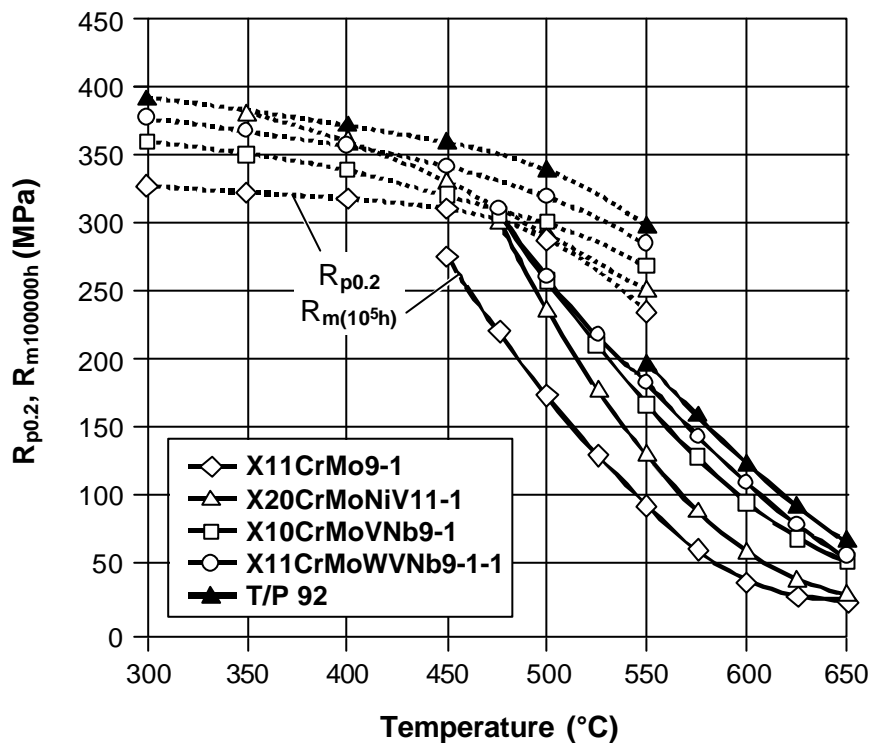

Figure 5: Strength properties of 9-12% Cr- steels.

After a period of standstill, the material development was reactivated by work carried out in the USA and Japan in the mid seventies (2). The prototype of the new steels from this development work is the modified 9% Cr steel T/P91 (EN designation: X10CrMoVNb9-1) invented in the USA (3,4). Meanwhile this steel is well known and applied in power plants all over the world. It is used in new plants as well as in refurbishment work of high pressure/high temperature piping systems. Although the carbon content is lower, the creep rupture strength of T/P91 is distinctly higher than that of X20CrMoNiV11-1. This has been achieved by alloying

with vanadium and niobium. T/P91 uses the precipitation of finely dispersed Nb/V-carbonitrides of type MX as additional strengthening effect. It was essential to balance the composition, because an optimum dispersion and particle size of MX can only be achieved by an optimized Nb/V- ratio and nitrogen content.

Subsequently new steel grades have been developed on the basis of T/P91, like X11CrMoWVNb9-1-1 (T/P911), T/P92 and T/P122 (2). These steel grades represent the current state of development for creep resistant ferritic steels. Their properties and application will be discussed in more detail in the following.

Current Developments for Advanced Power Plants

As mentioned before, improved economic efficiency has always been the major driving force behind the development of power plant technology. Economic benefits can be achieved by cost reductions due to operating larger unit sizes or to raise the plant efficiency. Both has been done in the past. Nowadays the issue of raising plant efficiency has gained increasing importance in view of the world-wide efforts to reduce CO_2 emissions.

Increasing plant efficiency is primarily a question of thermodynamics. Figure 6 shows how plant efficiency can be increased by raising the main steam pressure and temperature. With reference to the condition 535°C/185 bar, efficiency is increased by about 1.9% by increasing the pressure to 300 bar and 5.7% by increasing the temperature to 650°C. A combined increase of pressure and temperature leads to a rise in efficiency of more than 8%. As the example shows, improvement in plant efficiency can mainly be achieved through an increase in steam temperature.
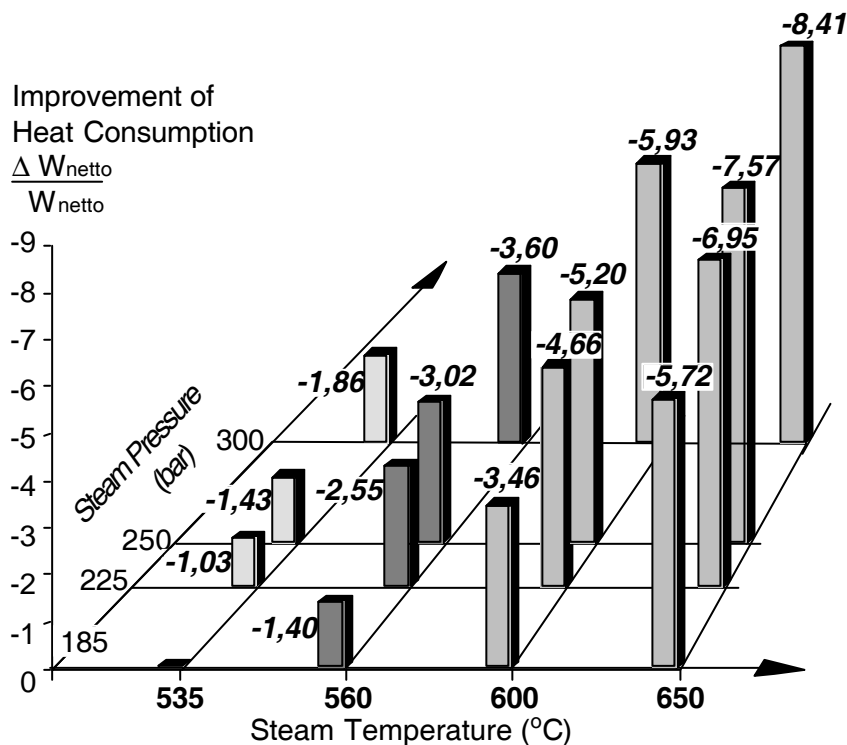

Figure 6: Increase of plant efficiency with increasing steam parameters.

However, this theoretical increase of efficiency can only be achieved, if suitable materials with sufficient creep strength are available to endure higher pressures and temperatures. Figure 7 shows how the increase of steam parameters is related to the creep rupture strength of the pipe material. The same initial conditions were chosen as in Figure 6. It is assumed that a unit operating at a steam pressure of 185 bar and a steam temperature of 535°C can be constructed by using 11CrMo9-10 (P22), which is a reasonable assumption. If stress or temperature is increased, a material with a higher creep rupture strength is needed. Considering again a pressure increase to 300 bar, 11CrMo9-10 has to be replaced by X20CrMoNiV11-1. A rise in steam temperature to 600°C requires the substitution by X10CrMoVNb9-1 (P91) for steel 11CrMo9-10. In case pressure and temperature are both increased, a creep resistant austenitic steel such as X3CrNiMoN17-13 (TP 316N) would be required. Austenitic steels, however, can only be used in power plant construction when their unfavorable physical properties do not impair the flexibility of operation of the unit. The impairment resulting from the use of an austenitic steel, in turn, depends on the component in question. For thick section components, such as headers and fittings in a main steam line, the use of austenitic steels is not appropriate, because the poor thermal conductivity and large coefficient of thermal expansion of these materials limit the startup and shutdown rates. Also the large expansions that occur with these materials can, if at all, only be managed by means of expensive design modifications. For such thick wall components, martensitic steels would be an appropriate choice. The steels must have not only adequate creep rupture strength but also good fabricability (e.g. hot workability, weldability and hot bending) because of the large section sizes involved.
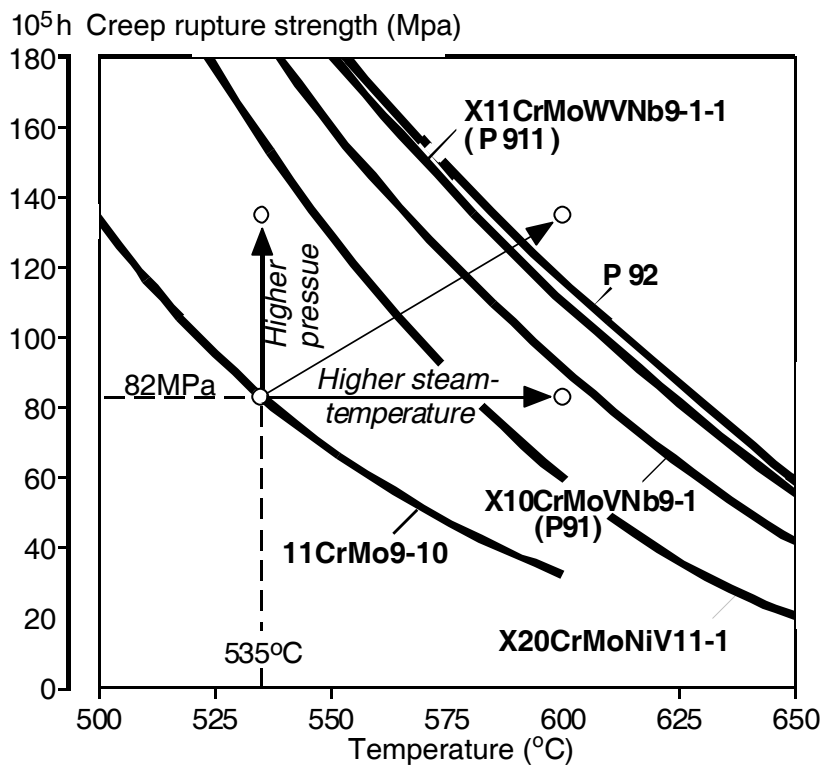

Figure 7: Requirements for creep rupture strength with increasing pressure and temperature.

For thin-wall components, attention should be paid to the fact that the metal temperature will be about 30 K higher than the steam temperature. The steel selected must have adequate creep rupture strength at the increased metal temperature. In addition, the steel must have adequate oxidation resistance. This requirement makes the 9% Cr steels, e.g. X10CrMoVNb9-1,

unsuitable for use as flue gas heated boiler tubes at steam temperatures in excess of 580°C. The thin wall of these components and the design of the equipment, however, enable austenitic steels to be used for this application without impairing the operational flexibility of the unit.

Steels for Pipework Applications

As the steam parameters and unit size increase, the pipe sizes increase, too. However, there are limitations in size due to production, fabricability, and flexibility of operation. Therefore each material has its limit of application. As for coal-fired power stations X20CrMoNiV11-1 has reached its limit in the 509 MW German unit Staudinger 5 (net thermal efficiency: 43%). The highest efficiencies of P91 (X10CrMoVNb9-1) have been reached with 47% in the Danish 425 MW units Nefo and Skaerbaek. A further increase in thermal efficiency through enhanced steam parameters could only be possible by the use of new, improved materials for pipework application.

The major part of work directed to the development of such new steels has been carried out in Japan and Europe. The most prominent Japanese steels NF 616 and HCM 12A have been standardized in ASTM/ASME as P/T92 and T/P122, respectively (see Table I) (2,5). The basic composition of those steels corresponds to that of T/P91. Their special feature is that they contain about 2% tungsten, and they are alloyed with boron, too. In order to avoid the formation of δ-ferrite in the microstructure, the molybdenum content of these high-tungsten steels has been reduced to about 0.5%. For T/P122 the chromium content has been raised to about 12% in order to improve the oxidation resistance. The increased chromium content, however, influences the phase stability so that 0.9% copper was added to get a nearly fully martensitic microstructure. X11CrMoWVNb9-1-1 (T/P911) has been developed by the work carried out in Europe as part of the COST 501 WP11 project, entitled "Advanced Materials for Power Engineering Components - High Efficiency, Low Emission Systems" (6). Its chemical composition is essentially the same as that of T/P91, except that it contains 1% tungsten additionally and also some boron.

T/P911 and T/P92 are currently the focal point of interest in Europe. They are intended for use in main steam lines. On the other hand T/P122 is more preferred for use as boiler components because of its higher oxidation resistance. It is not favored for use as thick section components. The disadvantages of T/P122 are mainly found in the area of fabricability. Due to the high copper content, its low A_{C1b} temperature entails longer tempering times at lower temperatures when the steel has to be tempered after hot working and welding. The same applies to the final heat treatment after pipe production. Moreover, it appears that, under the conditions of creep, the softening of the HAZ in such a copper-bearing steel tends to be more pronounced than it is usually known with 9-12% chromium steels.

T/P911 and T/P92 differ only in their molybdenum and tungsten contents, while the molybdenum equivalent (Mo + 1/2 W) of both steels is nearly the same. Tungsten has been added as an additional hardening element. First it was believed that tungsten mainly acts in solution hardening due to its large atomic size. However, it has been found out later that most of the tungsten content will precipitate as Laves phase during service operation. The benefit of boron is believed to decrease the coarsening rate of carbides.

The final heat treatment for both T/P911 and T/P92 consists of normalizing and tempering. An austenitising temperature of about 1060°C is adopted for hardening. A fully martensitic structure is obtained upon cooling to room temperature over a wide range of cooling rates. The Continous Cooling Transformation (CCT) diagram of T/P911, shown in Figure 8, is essentially

the same as that of T/P91 and T/P92. The M_s and A_{C1b} temperatures as well as martensite hardness are more or less the same for the three steels. And also the location of the ferrite-carbide transformation nose is comparable to that of T/P91.

Chemical composition, mass %	C	Si	Mn	P	S	Al	Cr	Ni	Mo	V	W	N	Nb
	0.115	0.200	0.51	0.017	0.002	0.007	8.85	0.24	0.94	0.22	0.95	0.084	0.069

Austenitizing temperature: 1060 °C
Holding time: 30 min.
Grain size: ASTM 9

A_{C1b} = 805 °C

A+C Austenite + Carbide
F+C Ferrite + Carbide
M   Martensite
M_S Martensite start temp.
M_F Martensite finish temp.
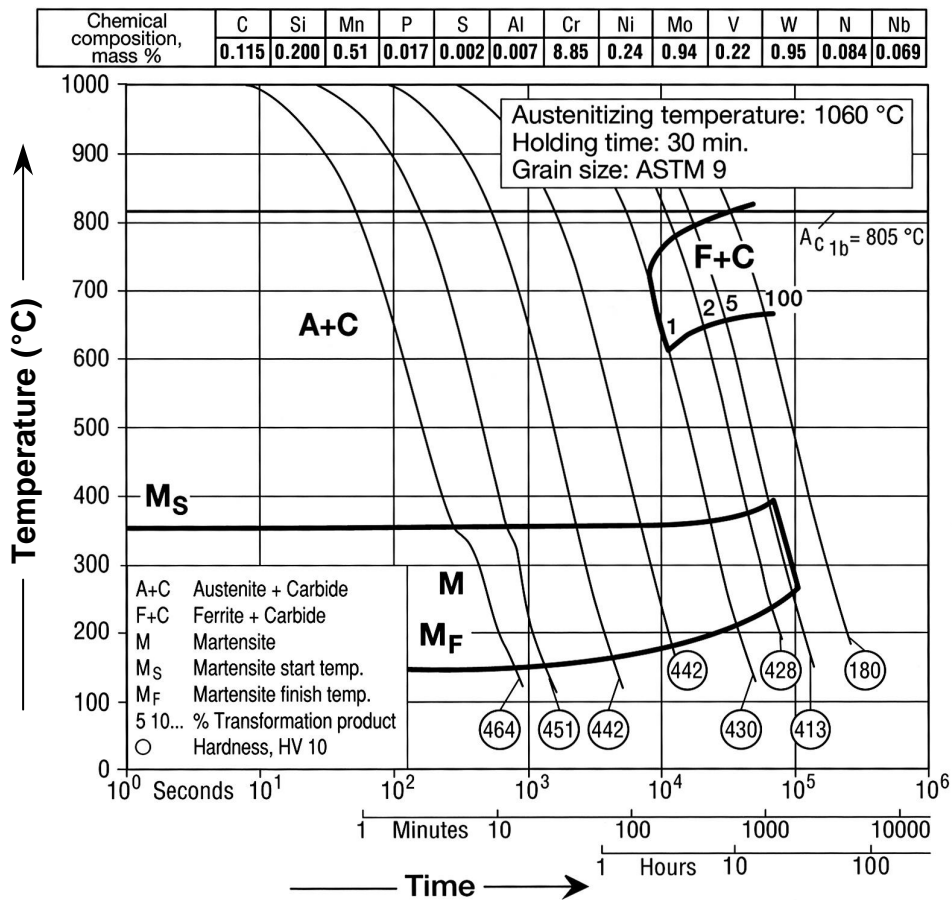5 10... % Transformation product
O   Hardness, HV 10

Figure 8: CCT diagram for X11CrMoWVNb9-1 (T/P911).

After normalizing T/P911 and T/P92 are tempered in the range 750 to 780°C which gives the right combination of high yield and tensile strength with good notch impact toughness. The microstructure of T/P911 in the normalized and tempered condition is shown in Figure 9.

As can be seen from the optical micrographs on the top of the figure 9, the transformation product is lath martensite. The austenite grain boundaries and lath boundaries are decorated with $M_{23}C_6$ particles. The numerous fine MX particles, rich in niobium and vanadium, cannot be recognized in these optical micrographs. They can only be noticed in electron micrographs (extraction replicas) associated with higher magnifications. The thin foil electron micrograph at the bottom-right of the figure shows the high dislocation density, typical of martensitic structure. In the as-heat treated condition, which is represented by the above micrographs, the steel does not contain any Laves phase. The Laves phase will not precipitate until the material is subjected to service conditions. Equilibrium phase diagrams calculated for T/P911 and T/P92 using the Thermo-Calc program show that both the steels have exactly the same phases (7). The only difference between them consists in the higher Laves phase content of T/P92, which can be attributed to its higher tungsten content.
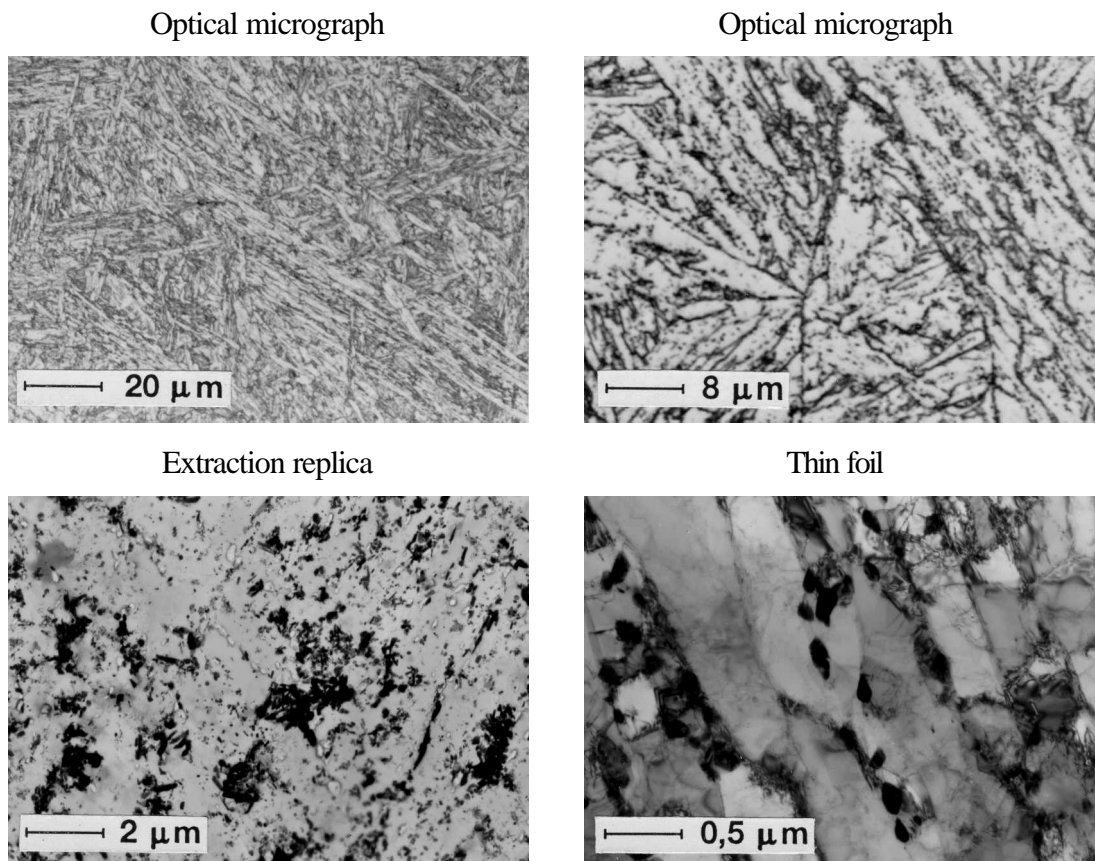
Figure 9: Microstructure of X11CrMoWVNb9-1-1 (T/P911).

The mechanical properties of both steels are also comparable, as could be expected. For instance, their hot yield strength values overlap (Figure 10). The slightly higher minimum values for T/P92 in the intermediate temperature range is merely the result of higher yield strength values determined on thin wall tubes of this material. However, those higher values can be attributed to a higher austenitizing temperature (1100°C) used for these components. The fact that all the measured values for T/P911 are above the mean curve for T/P92 also indicates that both steels have comparable strength properties.

The creep rupture strength had been a matter of controversy in the past. Figure 11 shows the current status of creep rupture tests carried out at our own research institute MFI (Mannesmann Forschungsinstitut) on T/P911 at 550, 600 and 650°C. Some additional tests were carried out at 575 and 625°C. The longest test duration so far has been about 76,000 h. The mean curves shown in the figure have been obtained by a graphical assessment method, widely used in Germany. All the data obtained in the COST 501 program have been included in the assessment. The data have been obtained from a total of 12 materials originating from seven casts, the total testing time being more than 1.4 million hours. All the experimental data are within a scatterband of ± 20% from the mean stress. The 10^5h- creep rupture strength obtained by extrapolation is 108 MPa at 600°C. This value is about 20% higher than that for T/P91.
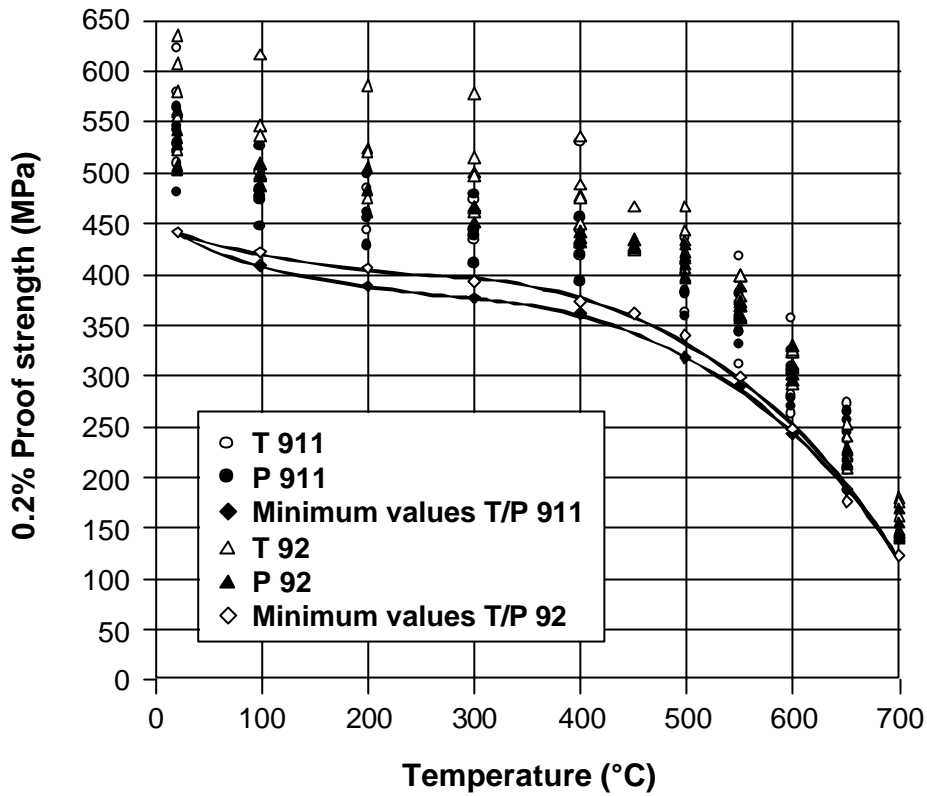
Figure 10: 0.2% proof strength values of T/P911 and T/P92 at elevated temperatures.
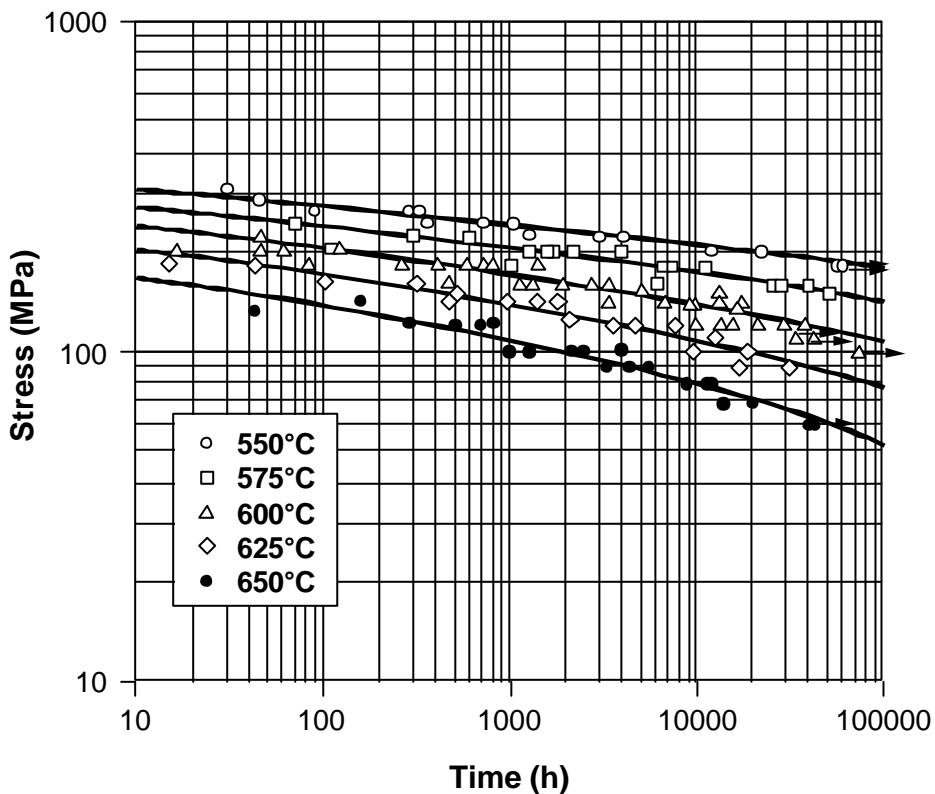

Figure 11: MFI creep tests on T/P911.

Most of the experimental data for P 92 originated from Japanese work. The longest test duration reported is about 55,000h (15). The 10^5h- creep rupture strength of 132 MPa at 600°C, which served as the basis for the ASME standardization, has been obtained by a Larson-Miller parametric assessment. This value is considerably higher than that for T/P911, although

both steels have comparable chemistry and mechanical properties. The main reason for this discrepancy is the fact that the T/P92 data were assessed by a method that is not applicable to the type of steels under consideration (8). A recent assessment made at MFI using presently the world's largest available database has determined the 10^5h- creep rupture strength of T/P92 at 600°C to be 116 MPa. This value is an agreement with 115 MPa reported by Ennis (9), using a completely different method based on the analysis of minimum creep rates.

Both T/P911 and T/P92 are produced by V&M (Vallourec&Mannesmann Tubes). Figure 12 shows the results of creep rupture tests of V&M on T/P92 carried out at 550, 600 and 650°C. The figure contains not only data determined at MFI but also data from CEV (Centre de Recherche Vallourec). Additional data for 575 and 625°C are available for this steel.
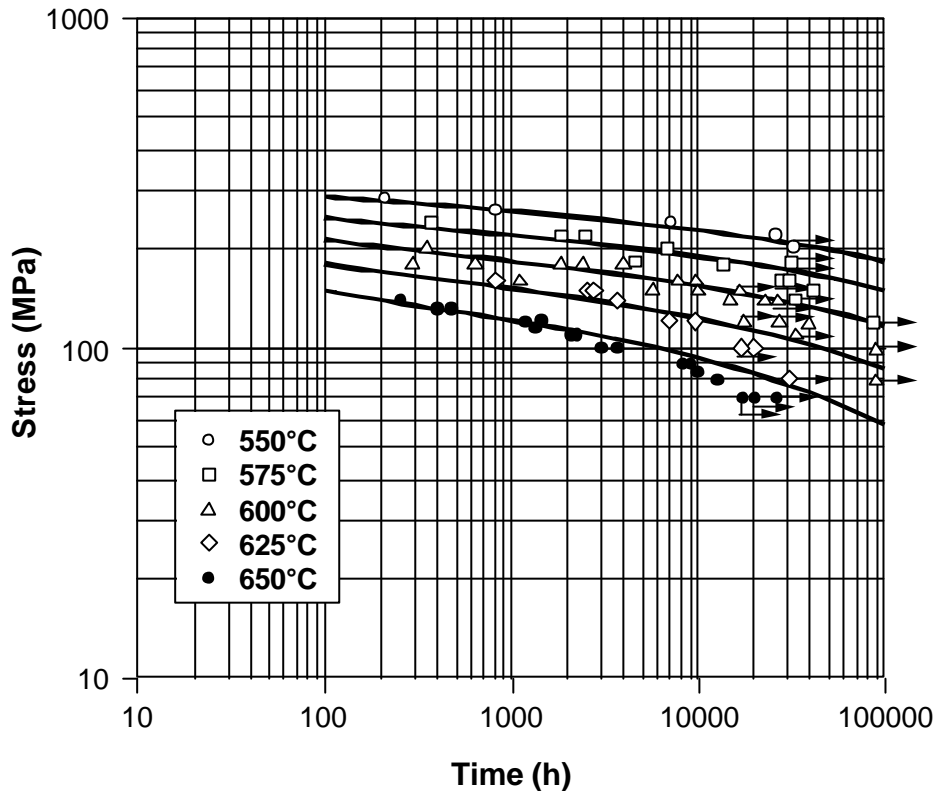

Figure 12: V&M creep tests on T/P92.

The data points at the longest test duration of more than 80,000 h belong to a pipe made by Nippon Steel. All other data points have been determined on V&M products. The longest test duration for these products is more than 30,000h. Mean curves have been obtained by the above-mentioned graphical assessment method. The difference in creep rupture strength between T/P911 and T/P92 is so small that their scatterbands widely overlap each other.

As regards fabricability, such as weldability and response to bending, there is not much difference between E 911 and P 92. Their behaviour also does not differ much from that of T/P91. MFI and V&M have gained considerable experience with T/P911 (10) and also with T/P92 (11). In addition much data for T/P911 is available from the COST 501 project (6,12). Data on the fabricability of T/P 92 can also be taken from the work published by Japanese researchers (13,14).

As in the case of P91, induction bends made of P911 and P92 have to be completely new normalized and tempered after bending. This is necessary to obtain the same creep strength as for unbent pipes. An example showing this is given by Figure 13.
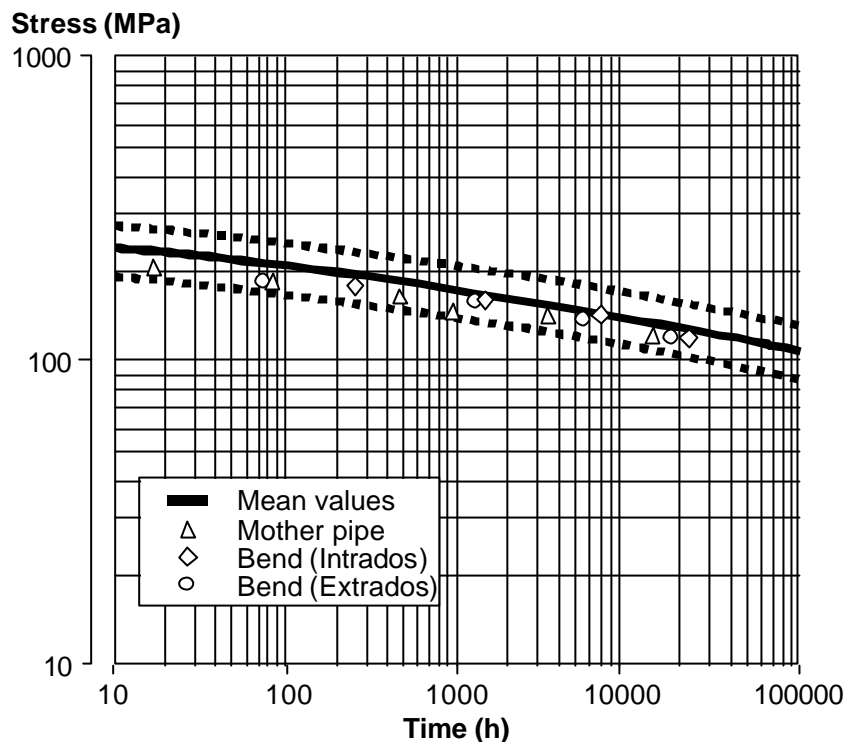
Stress (MPa)

Figure 13: Creep rupture strength of a P911 induction bend at 600°C.

A typical example for the creep behavior of a P911 weld at 600 and 650°C is shown in Figure 14. Short time tests at 600°C and high stresses lead to ruptures in the base material close to those for the mean line of the base material. With increasing test duration, however, creep rupture strength of the weld drops below the scatterband of the base material. Parallel to this drop the rupture location is shifted to the heat affected zone (HAZ). A similar behavior is found at 650°C, but at this temperature the drop occurs earlier. A maximum drop of about twice the size of the scatterband is observed. Occasionally ruptures are found in the weld metal. However, in all cases those ruptures were inside the scatterband. This creep behavior has to be taken into consideration in the design of piping systems, especially in cases where high stresses from the system are acting transverse to the weld seam. Again comparable behavior is also found for T/P92 and T/P91 welds.

To obtain preliminary information about the behaviour of the new steels in service, a few components made of these steels have been installed in existing Danish and German power plants (Table II). The validation of the two steels has attained a level that enables them to be used in the power plants on a large industrial scale. The components of the main steam lines in the power plant Niederaussem in Germany are made of P911 and those in the Danish plant Avedoere are made of P92. Both power plants are currently under construction.
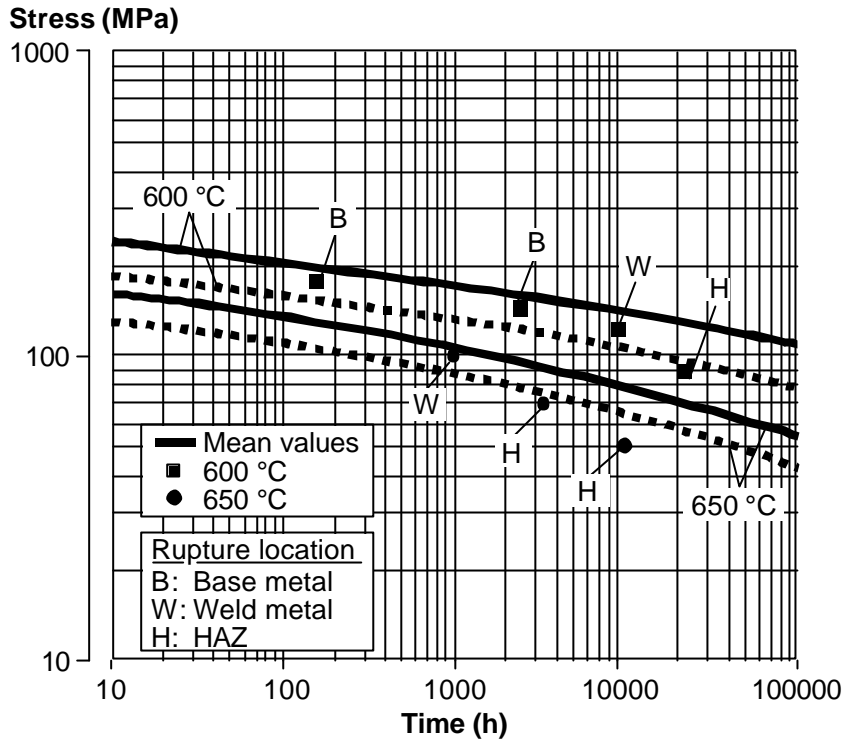
Figure 14: Creep rupture strength of a P911 weld at 600 and 650°C.

Table II Application of new tungsten bearing steels in danish and german power stations

Power Station	Material Grade	Size (mm)	Component	Steam Conditions	Installation
Vestkraft Unit 3 (Denmark)	P92	ID 240x39 (56)	straight pipe main steam	560°C/250bar	1992
Nordjyllands-vaerket (Denmark)	P92 P122	ID 160x45	header	582°C/290bar	1996
Schkopau Unit B (Germany)	P911	ID 550x24	induct. bend hot reheat	560°C/70bar	1996
Staudinger Unit 1 (Germany)	P911	ID 201x22	induct. bend main steam	540°C/213bar	1996
Skaerbaek Unit 3 (Germany)	P911	ID 230x60	induct. bend main steam	582°C/290bar	1996
GK Kiel (Germany)	P92	ID 480x28	header	545 C/53bar	1997
VEW (Germany)	P911	OD 31.8x4	superheater	650 C	1998
Westfalen (Germany)	P911 P92	ID 159x27	steam loop (test facility)	650°C/180bar	1998

Steels for Waterwalls

The scope to enhance steam parameters will be limited, if the pressure and temperature in the waterwalls cannot be increased simultaneously. The necessary increase in the temperature would entail a changeover from the time-independent to the time-dependent design stress.

Bainitic-ferritic steels, such as 10CrMo4-5 (T12) and 11CrMo9-10 (T22), which have been used so far, do not have adequate creep rupture strengths for use in waterwalls under the conditions of advanced power plants (Figure 15). Using 13CrMo4-5 an allowable wall temperature of about 500°C is obtained for the given tube dimensions 38OD x 6.3mm WT and a design pressure of 350 bar which corresponds to a live steam pressure of approximately 300 bar. However, wall temperatures around 525°C will be expected. The situation would not change by the use of 11CrMo9-10 material. From the viewpoint of creep strength T91 (X10CrMoVNb9-1) would seem to be a suitable solution. As a requirement of manufacturing waterwalls cannot be subjected to a post-weld heat treatment after welding. However, martensitic 9-12% Cr steels attain a maximum hardness between 450HV10 (e.g. T91) and 650 HV10 (e.g. X20CrMoNiV11-1) in the as-welded HAZ, depending mainly upon the carbon content. A reduction of carbon content in those steels is only possible to a limited extent for reasons of microstructural stability. Such high hardness levels are not acceptable, mainly because of the risk of stress corrosion cracking. Therefore the high strength 9-12% Cr steels are not suitable for use in waterwalls.
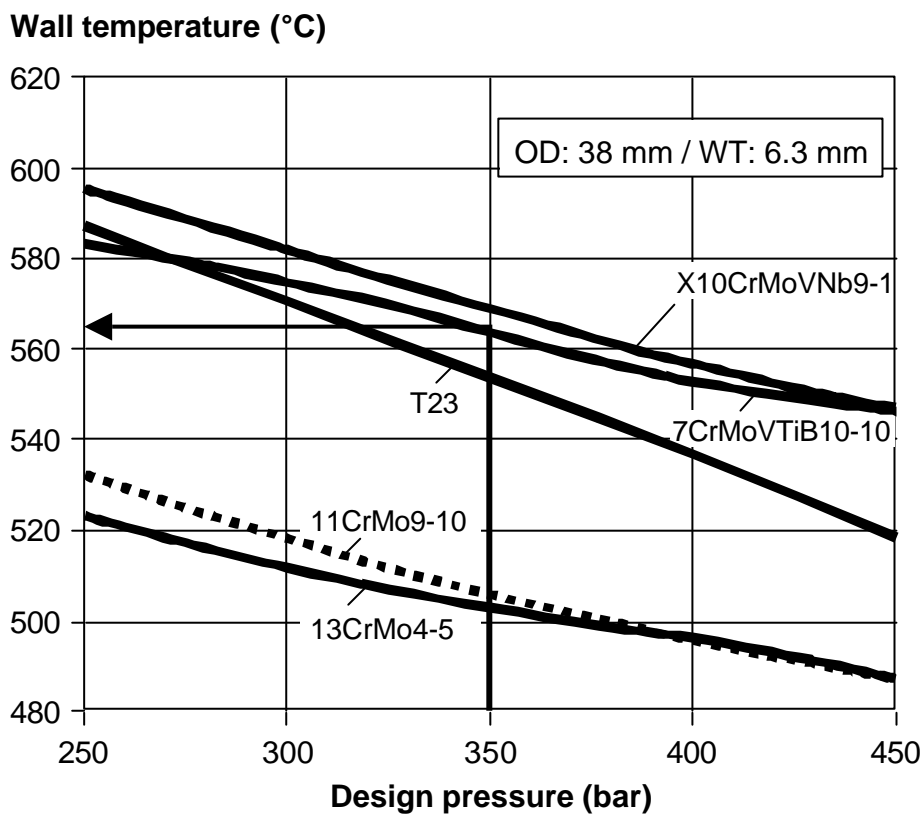
Wall temperature (°C)

Figure 15: Allowable temperatures for different waterwall materials.

The aspect of hardness had to be taken into account when developing new steels. As shown in Figure 15 the new steels T23 and 7CrMoVTiB10-10 (T24) allow high enough wall temperatures. The steels have been developed in Japan (T23) and Germany (T24). They are both based on 11CrMo9-10. Thanks to their lower carbon content, the maximum hardness in the HAZ lies at 350- 360 HV10. The steels are micro-alloyed with vanadium, niobium, titanium and boron to achieve a high creep rupture strength (see Figure 4). T23 also contains tungsten, while its molybdenum content is considerably reduced (see Table I). The applied hardening mechanisms are basically the same as have been used for the new 9-12% Cr steels. Due to their origin, however, most of the other properties of T23 and T24 are similar to T22 (11CrMo9-10). They belong to the group of CrMo- steels with a predominantly bainitic microstructure. As an example Figure 16 shows the transformation behavior of T24. The main

difference to the transformation behavior of T22 is the retardation of ferrite formation which is caused by the micro-alloying additions. Due to their high cooling rate, thin-wall tubes used in membrane walls exhibit a bainitic martensitic structure. Both steels are used in a normalized and tempered condition.

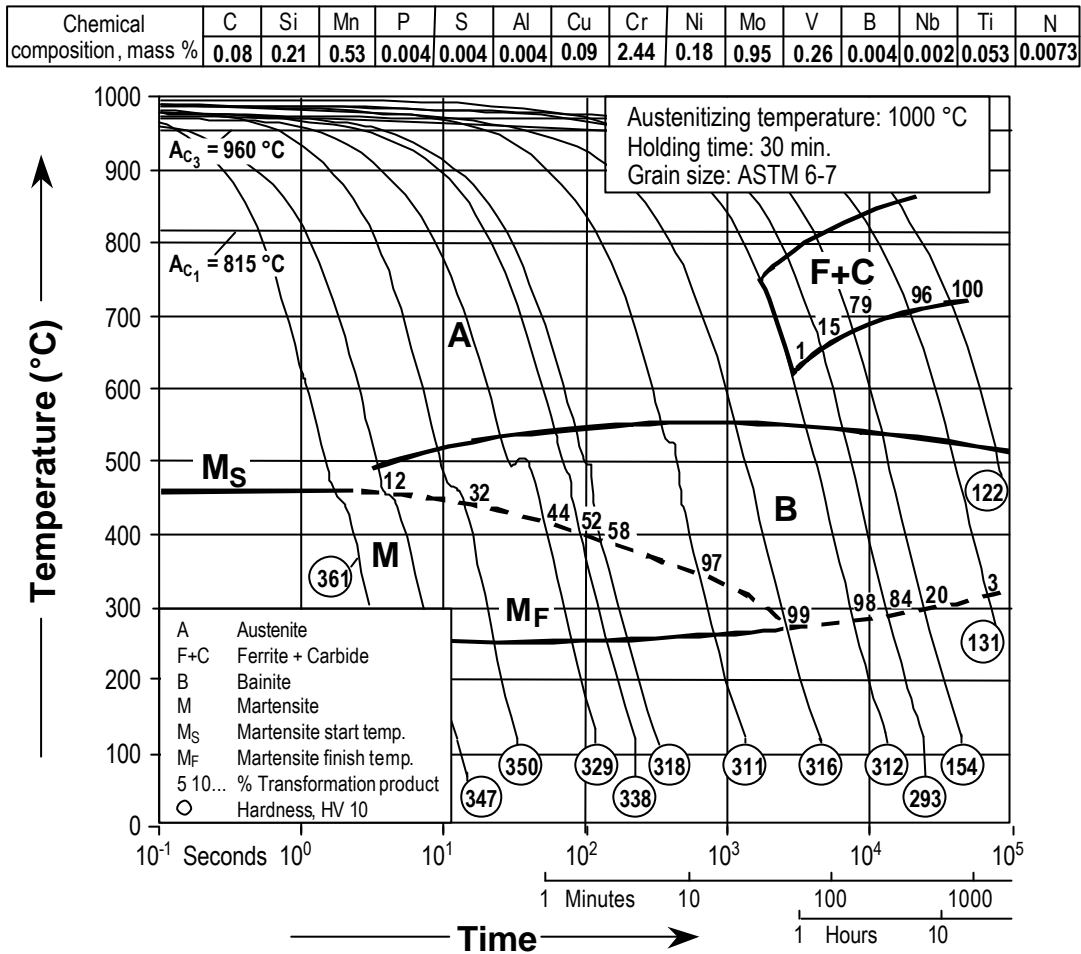| Chemical composition, mass %	C	Si	Mn	P	S	Al	Cu	Cr	Ni	Mo	V	B	Nb	Ti	N
	0.08	0.21	0.53	0.004	0.004	0.004	0.09	2.44	0.18	0.95	0.26	0.004	0.002	0.053	0.0073

Figure 16: CCT diagram for 7CrMoVTiB10-10 (T/P24).

A user of T23 and T24 can find a compilation of the most important properties in Ref. (15). Additional data on T23 are given in Ref. (16), whereas an extensive review of the current status of the German development 7CrMoVTiB10-10 (T24) is provided in Ref. (17).

Test waterwall panels have been manufactured with the new steels and are tested in a number of Danish and German power plants (Table III). Predominately panels made of T23 and 7CrMoVTiB10-10 (T24) have been installed. In addition X10CrMoVNb9-1 (T91) and the Japanese steel HCM12 have been used, too. While the T91 panels were heat treated after welding, the martensitic ferritic steel HCM12 was used in the as-welded condition, like in the case of T23 and 7CrMoVTiB10-10. However, the HCM12 panels had to be removed after only a short time of operation due to cracks in the tubes.

Table III In-service tests of new materials for waterwalls

Power Station	Material	Dimensions (mm)	Component	Service Parameters	Installation
Heyden (Germany)	X10CrMoVNb9-1	OD 51 x 6.3 Division 70.67	evaporator	440°C steam, 240 bar	September 1993
Lippendorf, Unit F (Germany)	X10CrMoVNb9-1 HCM 12	OD 44.5 x 5.0 division 60	evaporator	332°C steam,133 bar	9/1993 removal HCM 12 March1994
Weisweiler, Unit G (Germany)	X10CrMoVNb9-1 HCM 12 7CrMoVTiB10-10	OD 26.9 x 5.0 division 65 (2 x 12 tubes)	evaporator parallel SH3	510°C steam, 160 bar	April 1994 removal HCM 12 May 1996
Asnaes, Unit 4 (Danmark)	HCM 12 T23 7CrMoVTiB10-10	OD 38 x 5.6 division 57 (10 tubes) OD 38 x 6.3 division 57 (2 x 5 tubes)	evapoarator	460°C steam, 228 bar	August 1995 June 1995
Neckar 2 (Germany)	X10CrMoVNb9-1 7CrMoVTiB10-10	OD 38 x 7.1 OD 38 x 6.3 division 100 (2 x 8 tubes)	evaporator	440°C steam, 280 bar	September 1996
Thierbach, Unit D (Germany)	7CrMoVTiB10-10	OD 26.9 x 5.0 division 65 meander (10 tubes)	parallel SH	480°C steam, 148 bar	July 1996
Ensted, Unit 3 (Danmark)	HCM 12	OD 38 x 6.3 division 45 4.2 x 2 x 10 m	SH - wall	500°C inlet 542°C outlet 211 bar	June 1997
Amager (Danmark)	HCM 12 T23	OD 31.8 x 5.6 meander (6 tubes) OD 38 x 6.3	inside boiler	1984 cycles, 50 K 575°C metal temp. 280 bar	May 1994 removal July1995 August 1995

In view of the excellent creep rupture strength, other applications were looked for. Outside of Europe T23 is used as tube material for reheaters and superheaters. Due to the low chromium content, however, this application is limited by oxidation and flue gas corrosion. But regarding application as pipe material in the main steam systems, corrosion will be of less importance. Especially 7CrMoVTiB10-10 could be an interesting alternative to P91 for use in conventional plants with steam temperatures up to about 545°C. That could be replacements in old plants as well as applications in new plants with conventional steam temperatures, e.g. in combined cycle plants. In order to allow such applications, thick wall components had to be tested. Figure 17 shows the current status of creep testing at 550°C on thick wall pipes and forgings compared to thin wall tubes and plates. While the thin wall products have already reached more than 100,000h, the longest duration of thick wall products is currently about 40,000h. All rupture points lie within the scatterband of the thin wall products.

It should be mentioned that a difference in heat treatment has proved to be necessary. Thick wall products have to be used in a water quenched and tempered condition. Otherwise the lower cooling rate leads to a microstructure with lower strength and toughness. The first commercial application of thick wall 7CrMoVTiB10-10 (P24) is in preparation. It will be used in the piping system of a small industrial power plant. Pipes have been produced with a wall thickness up to 45mm. The plant will go into operation in 2002.
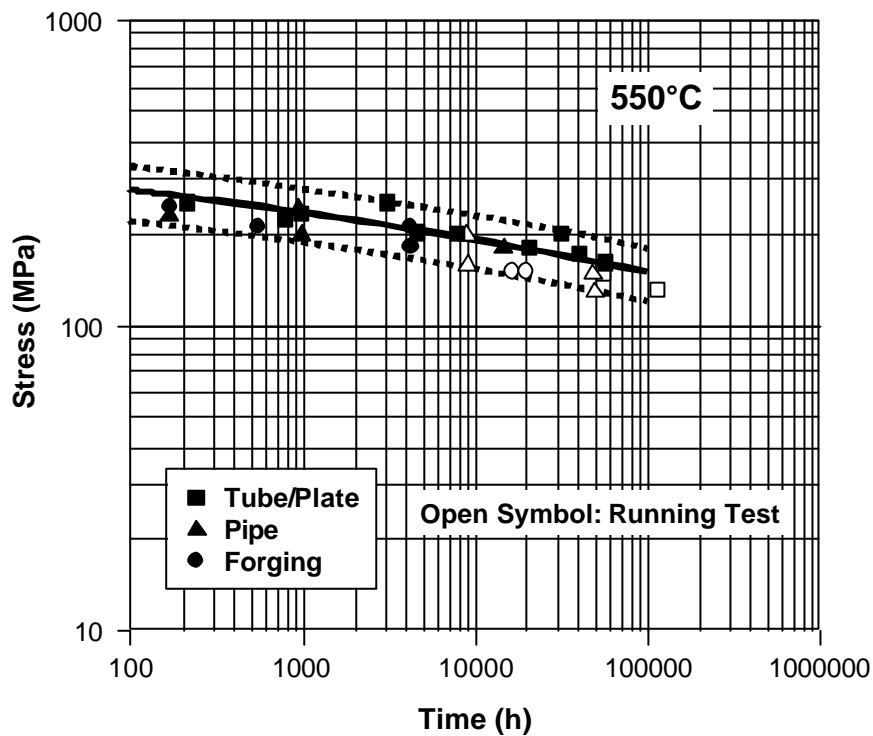

Figure 17: Creep tests on various product forms of Grade 24 (7CrMoVTiB10-10).

Outlook to the Future

With increasing steam temperature the lifetime of components will not only be limited by creep strength but also by oxidation and high temperature corrosion. In-service tests have shown that the newly developed steels T/P911 and T/P92 are not suitable for use as boiler tubes with a steam temperature of 600°C (18). In general 9% Chromium- steels have a distinctly lower oxidation resistance than 12% Chromium- steels, like X20CrMoNiV11-1 (19). The difference becomes most severe at temperatures above 600°C. As an example, Figure 18 gives results of

comparative tests on X20CrMoNiV11-1, X10CrMoVNb9-1 (T/P91) and T/P92 in steam. The results of Figure 18 show that 9% Cr- steels can not be used in steam lines outside the boiler, if the steam temperature is 650°C or over.

Currently world-wide research programs are heading for 650°C steam temperature as a next step to further improve plant efficiency. MFI is involved in such a program organized in Europe by COST 522. In the on-going first phase laboratory heats were produced and tested (Table IV).
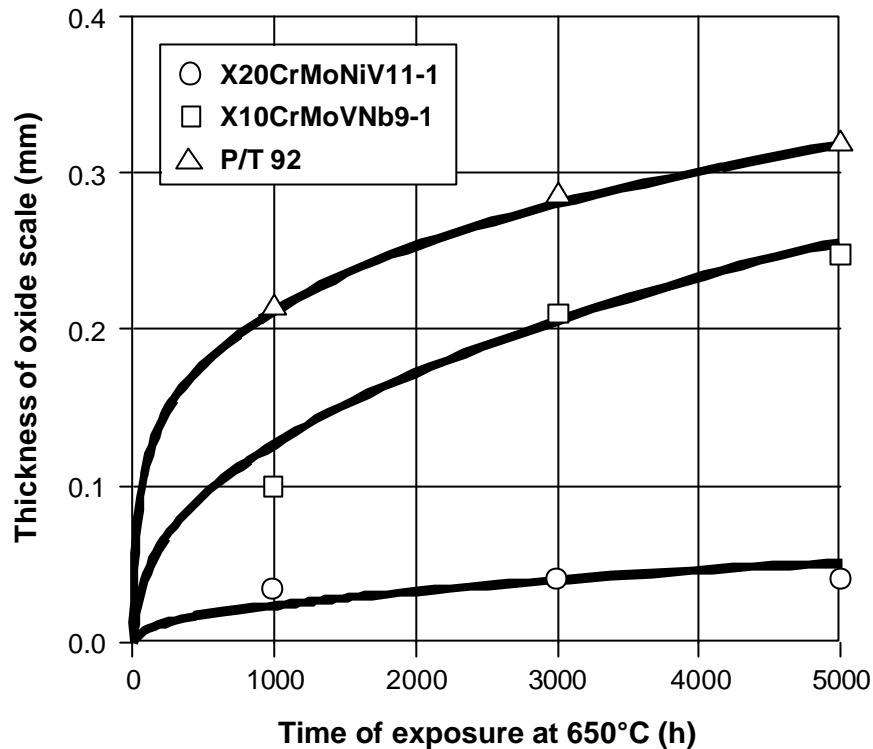

Figure 18: Steam oxidation of 9-12% Chromium- steels at 650°C.

Table IV Chemical composition of new 12% chromium- laboratory heats

Material	Chemical Composition (mass-%)										
	C	Si	Mn	Cr	Ni	Co	Mo	V	Nb	B	N
Heat A	0.190	0.10	0.52	11.64	0.20	0.01	1.48	0.26	0.058	0.0035	0.015
Heat B	0.184	0.10	0.51	11.54	0.25	0.01	1.48	0.26	0.058	0.0039	0.047
Heat C	0.158	0.09	0.53	11.25	0.26	0.90	1.46	0.25	0.047	0.0062	0.063
Heat D	0.160	0.10	0.50	11.42	0.26	1.06	1.48	0.25	0.058	0.0117	0.063
Heat E	0.129	0.10	0.49	11.29	0.28	3.06	1.44	0.25	0.057	0.0068	0.051

As mentioned before in the discussion on T/P122, phase stability did not allow the use simply of a 9% Chromium- steel and increase the chromium content. A single phase martensitic microstructure can only be achieved by simultaneously increasing the proportion of austenite forming elements, such as carbon, nitrogen, copper, nickel or cobalt. However, it has to be taken into account that other material properties, e.g. A_{C1b} temperature, will be influenced by

adding those elements. Based on a composition similar to T/P91, laboratory heats were produced with a chromium content > 11% and 1.5% molybdenum as well as different contents of carbon, nitrogen, cobalt and boron.

Figure 19 shows the current status of creep tests on those laboratory heats at a temperature of 625°C. For comparison the mean curve and scatterband of T/P911 is included in the figure. All rupture points lie between the mean curve and the upper limit of the scatterband. The highest creep strength values have been reached by heat E with 3% cobalt. Assuming that no steep decrease occurs at longer times, an increase of creep rupture strength by about 20% can be expected compared to T/P911. The disadvantage of this material is its high price due to the high cobalt content. Therefore a further optimization is planned with the aim of reducing the cobalt content but maintaining the creep strength
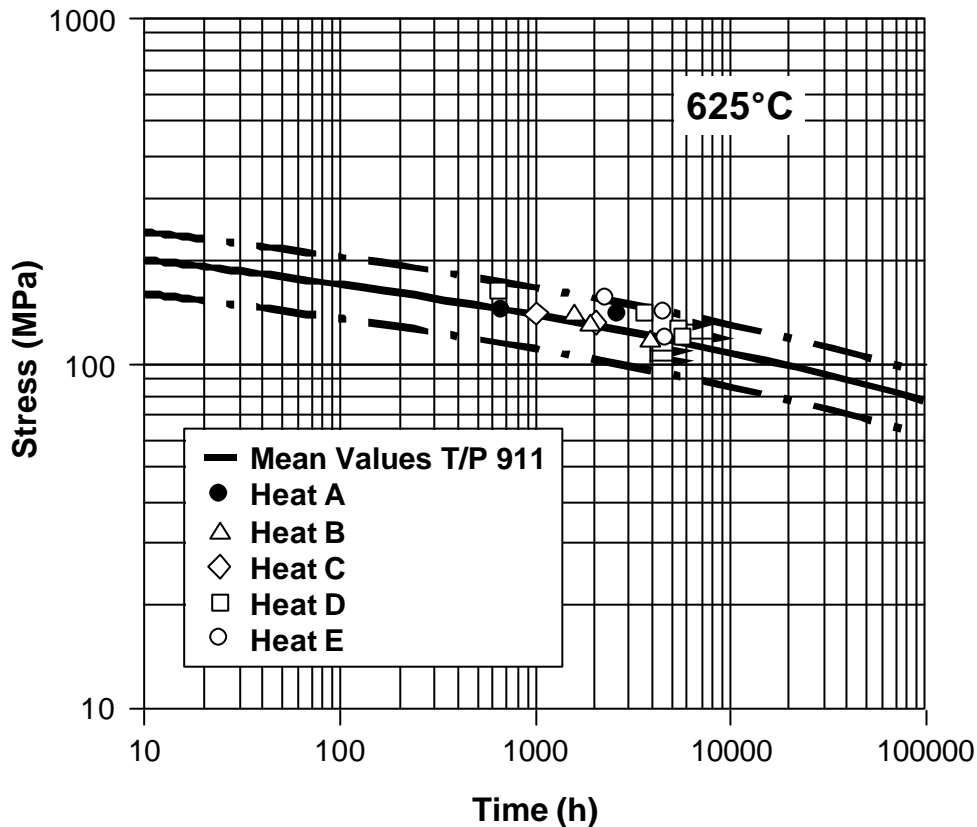

Figure 19: Creep tests on new 12% Cr- laboratory heats.

Figure 20 gives an overview on creep rupture strength of various materials with respect to temperature. This figure also gives a good overview on the present status of development of creep resistant steels for power plants. The newly developed steels T/P91, T/P911 and T/P92 have moved the application of ferritic steels into the range of austenitic steels. T/P911 and T/P92 will enable live steam and hot reheat lines to be operated at 605°C and 625°C, respectively.

The achievements which have been made can easily been demonstrated by a line drawn at 100MPa. The intersection of this line with the creep rupture strength curves gives an approximate value of the highest live steam application temperature of the respective material. A further increase is anticipated by the new 12%Chromium- steels which are under development. This will probably mark the limit for ferritc steels. There is only a small temperature range for a potential application of austenitic steels for live steam piping, which is

not reasonable to be used in view of the problems discussed before. However, the use of nickel-base alloys, e.g. Inconel 617, would enable the steam temperature to be raised considerably. The European research project THERMIE aims at developing power plants for a steam temperature of 700°C. Such a steam temperature will enable the plant efficiency to be raised beyond 50%. If the development progresses as planned, a 700°C power plant could be a reality by about 2015.
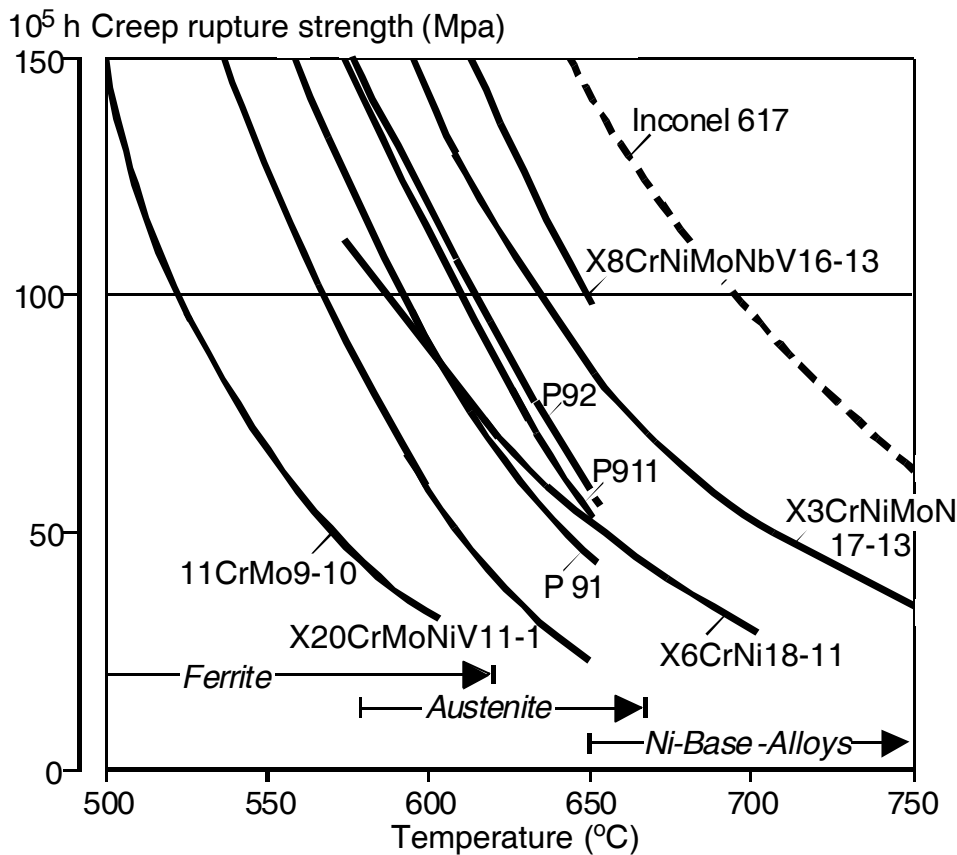

Figure 20: Materials for main steam pipes in power plants.

References

(1) G. Kalwa, "State of the Development and Application Techniques of the Steel X20CrMoV12-1," Nuclear Engineering and Design, 84 (1985), 87-95.

(2) R. Blum et al., "Newly Developed High-Temperature Ferritic-Martensitic Steels from USA, Japan, and Europe," VGB Kraftwerkstechnik (English Issue), 74 (1994), 553-563.

(3) V.K. Sikka, C.T. Ward, and K.C. Thomas, "Modified 9Cr-1Mo Steel – An Improved Alloy for Steam Generator Application," (Paper presented at conference Ferritic Steels for High-Temperature Applications, Warren, Pa., 6-8 October 1981).

(4) D.A. Canonico, "Thick-Walled Pressure Vessels for Energy Systems," (Technical Program and Data Package for Use of Modified 9Cr-1Mo Steel, ASME Sect. I and VIII, 7 April 1982).

(5) E. Metcalfe, ed., New Steels for Advanced Plant up to 620°C (Oxon, UK, PICA Publ. Services 1995), 200.

(6) M. Staubli et al., "European Collaborative Evaluation of Advanced Boiler Materials," <u>Proc. of 6th Liège Conference on Materials of Advanced Power Engineering,</u> eds. J. Lecomte-Beckers et al., Vol. I, (Forschungszentrum Juelich, 1988), 87-103.

(7) J. Hald, "Metallurgy and Creep Properties of New 9-12% Cr- Steels," <u>Proc. 18th Conf Langzeitverhalten warmfester Staehle und Hochtemperaturwerkstoffe</u> (VDEh, 1995), 40-51.

(8) W. Bendick and M. Ring, "Creep Rupture Strength of Tungsten Alloyed 9-12% Cr Steels for Piping in Power Plants," <u>Steel Research</u>, 67 (1996), 397-405.

(9) P.J. Ennis, "Creep Strengthening Mechanisms in High Chromium Steels," (Paper presented at 3rd EPRI Conference Advances in Materials Technology for Fossil Power Plants, Swansea, UK, 6-8 April 2001).

(10) W. Bendick, K. Haarmann, and M. Zschau, "E911 – A New Steel for Power Plant Steam Pipework," <u>VGB PowerTech</u> (5/2000), 87-91.

(11) D. Richardot et al., <u>The T92 / P92 Book</u> (Vallourec & Mannesmann Tubes, 2000), 68.

(12) H. Cerjak, E. Letofsky, and M. Staubli, "The Role of Welding for Components Made from Advanced 9-12% Cr- Steels," Vol. I, ibid. (6), 105-122.

(13) H. Naoi et al. "NF 616 Pipe Production, Properties, and Welding Consumable Development," in (5), 8-29.

(14) F. Masuyama and T. Yokoyama, "NF 616 Fabrication Trials in Comparison with HCM 12A," in (5), 30-44.

(15) J. Arndt et al., <u>The T23 / T24 Book – New Grades for Waterwalls and Superheaters</u> (Vallourec & Mannesmann Tubes, 1998), 50.

(16) F. Masuyama et al., "Development of a Tungsten Strengthened Low Alloy Steel with Improved Weldability," <u>Proc. Conf. Materials of Advanced Power Engineering 1994,</u> eds. D. Coutsouradis et al., Dordrecht, (Netherlands, Kluwer Academic Publ., 1994), 173-181.

(17) R.U. Husemann, W. Bendick, and K. Haarmann, "The New 7CrMoVTiB10-10 (T24) Material for Boiler Waterwalls," (ASME PWR-Vol. 34) 633-640.

(18) K. Zabelt et al., "Properties and Application Limits for Thin-Walled and Thick-Walled Components of Heat Resistant Steels NF 616 and P92," <u>VGB PowerTech</u> (5/2000), 92-96.

(19) W.J. Quadakkers and P.J. Ennis, "The Oxidation Behavior of Ferritic and Austenitic Steels in Simulated Power Plant Service Environments," Vol. I, ibid. (6), 123-138.